Study of barrier distribution function for $^{40}Ca + ^{90}Zr$ fusion reaction within channel coupling approach

Summer Student Program 2015 at JINR

Flerov Laboratory of Nuclear Reactions

Fyodorov S.V.
Omsk state university
Faculty of physics

Supervisor: Karpov A.V.

Dubna 2015

Contents

1. Introduction

The near-barrier fusion of nuclei remains still to be one of the most interesting phenomena in nuclear reactions studies. The dynamics of low-energy fusion is governed by quantum tunneling through a Coulomb barrier occurring under conditions where relative motion is strongly coupled to internal degrees of freedom primarily, to vibrations of nuclear surfaces, rotation of deformed nuclei, and nucleon transfer [1].

One of the important characteristics of the near-barrier fusion is so-called barrier distribution function (see it definition below). It can be obtained from the experimental data on quasi-elastic scattering as well as on the fusion cross section. The second way has been used in this work. The main difficulty is to calculate a value, which is called the transmission probability. It can be obtained from three models, they are Single-Barrier Penetration Model, Empirical [2] and Quantum Channel Coupling (QCC) Model.

The barrier distribution function was already extensively studies in literature [1,3]. However, this quantity (in particular, nature of its structure), is far from complete understanding. The standard approach for study near-barrier fusion reactions is the QCC one [4,6,9]. This model has one weakly defined parameter, namely the number of accounted phonons of the collective modes included into the computational scheme.
Thus, the aim of this work is to:

- Study the influence of different collective excitation modes on the sub-barrier fusion.
- Study of the phonons number effect on the barrier distribution function behavior.
- Study of the barrier distribution function asymptotic behavior when the number of phonons tends to infinity.

The calculations were performed with the use of the web knowledge base NRV [4], which is described in Sec. 2. The used models are discussed in Sec. 3. Section 4 contains the results of our calculations, including a comparison with experimental data. In Sec. 5 we summarize our results and present our conclusion.

2. NRV - Low Energy Nuclear Knowledge Base

All the calculation shown in this paper are done within the web knowledge base on low-energy nuclear physics (NRV)[4]. NRV is an open and permanently extended global system of management and graphical representation of nuclear data and video-graphic computer simulation of low-energy nuclear dynamics. It consists of a complete and renewed nuclear database and well-known theoretical models of low-energy nuclear reactions altogether forming the "low-energy nuclear knowledge base". The NRV solves two main problems.

1. Fast and visualized obtaining and processing experimental data on nuclear structure and nuclear reactions.
2. Possibility for any inexperienced user to analyze experimental data within reliable and commonly used models of nuclear dynamics.

The system is based on the realization of the following principal things:

- The net and code compatibility with the main existing nuclear databases.
- Maximal simplicity in handling: extended menu, friendly graphical interface, hypertext description of the models, and so on.
- Maximal visualization of input data, dynamics of studied processes and final results by means of real 3-dimensional images, plots, tables and formulas, and a 3-dimensional animation.

3. Models

Single-Barrier Penetration Model

The potential of interaction of two nuclei is shown in fig. 3.1. The maximum, which correspond to point R_b called Coulomb barrier. Position of this maximum usually larger by 1 or 2 fm than the sum of nuclear radii $R_1 + R_2$. At low near-barrier energies the light and/or medium colliding nuclei having overcome the Coulomb barrier and coming in contact are captured in the potential pocket and fuse (form a compound mono-nucleus).

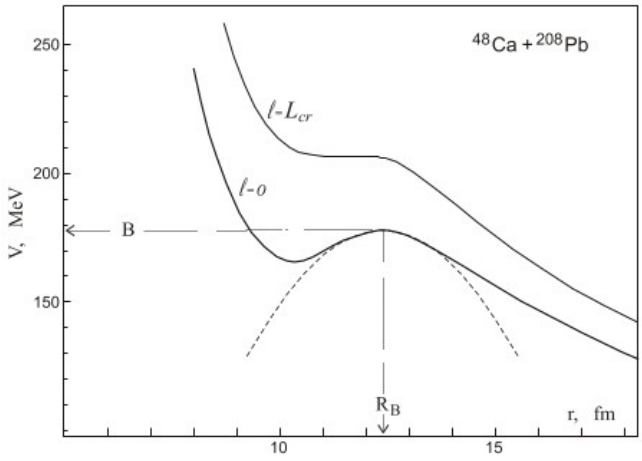

Fig. 3.1 Interaction of two spherical nuclei $^{48}Ca+^{208}Pb$. The proximity potential is used here for the nuclear interaction. Dashed curve shows the parabolic approximation of the Coulomb barrier. For the partial wave $l=L_{cr}$

The fusion cross section can be decomposed over partial waves.

$$\sigma_{fus}(E)=\frac{\pi\hbar^2}{2\mu E}\sum_{l=0}^{\infty}(2l+1)T_l(E) \quad , (1)$$

where μ is the reduced mass of the system, E is the center-of-mass energy, and $T_l(E)$ is the partial barrier transmission probabilities. The transmission probabilities can be calculated by solving one-dimensional Schrodinger equation with appropriate (non-reflective) boundary condition. The Hill-Wheeler formula [5] for the transmission probabilities can be used approximating the barrier radial dependence by a parabola .

$$T_l^{HW}(B;E)=\left[1+\exp\left(\frac{2\pi}{\hbar\omega_B(l)}\left[B+\frac{\hbar^2}{2\mu R_B^2(l)}l(l+1)-E\right]\right)\right]^{-1} \quad . (2)$$

Here $\hbar\omega_B=\sqrt{\hbar^2/\mu|\partial^2 V/\partial r^2|}$ is defined by the width of the potential barrier, B is the height of the barrier and $R_B(l)$ is the position of the effective barrier including a centrifugal term.

Interaction of Deformed and Deformable Nuclei [6]

The shape of axially deformed nucleus is defined as follows

$$R(\bar{\beta},\theta)=\widetilde{R}\cdot\left(1+\sum_{\lambda\geq 2}\beta_\lambda\sqrt{\frac{2\lambda+1}{4\pi}}P_\lambda(\cos(\theta))\right) \quad , (3)$$

where $\bar{\beta}\equiv\{\beta_\lambda\}$ are dimensionless deformation parameters of multi-polarity $\lambda=2,3,\ldots,P_\lambda$ are the Legendre polynomials. Potential energy of two deformable nuclei is the sum of the Coulomb, nuclear, and deformation energies

$$V_{12}(r;\dot{\beta}_1,\theta_1,\dot{\beta}_2,\theta_2)=V_C(r;\dot{\beta}_1,\theta_1,\dot{\beta}_2,\theta_2)+V_N(r;\dot{\beta}_1,\theta_1,\dot{\beta}_2,\theta_2)+ \\ +\frac{1}{2}\sum_{i=1}^{2}\sum_{\lambda}C_{i\lambda}\cdot(\beta_{i\lambda}-\beta_{i\lambda}^{g.s.})^2 \quad (5)$$

Here $i=1,2$ numerates the nuclei, $C_{i\lambda}$ are the surface stiffness parameters, and $\theta_{1,2}$ are the orientations of symmetry axes, see Fig. 3.2.

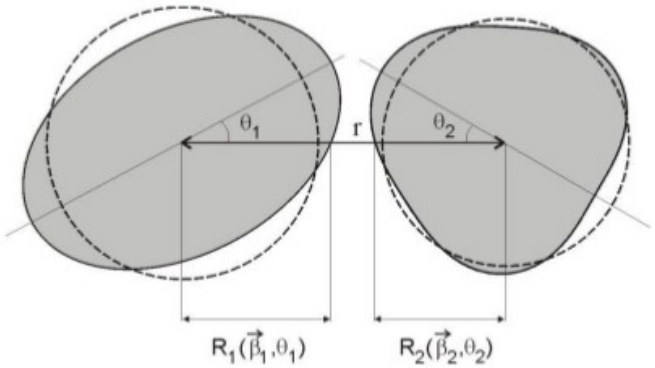

Fig. 3.2 Schematic picture of two deformed nuclei rotating in the reaction plane.

The Coulomb interaction of two deformed nuclei is given by

$$V_C = Z_1 Z_2 e^2 \left[F^{(0)}(r) + \sum_{i=1}^{2} \sum_{\lambda \geq 2} F_{i\lambda}^{(1)}(r) \beta_{i\lambda} Y_{\lambda 0}(\theta_i) \right] + \tag{5}$$

$$+ Z_1 Z_2 e^2 \sum_{i=2}^{2} \sum_{\lambda'} \sum_{\lambda''} \sum_{\lambda=|\lambda'-\lambda''|}^{\lambda=\lambda'+\lambda''} F_{i\lambda}^{(2)}(R) \, M \sum_{\mu} \int Y^{*}_{\lambda'\mu} Y^{*}_{\lambda''-\mu} Y_{\lambda 0} \, d\Omega \, \beta_{i\lambda'} \beta_{i\lambda''} Y_{\lambda 0}(\theta_i) + \ldots$$

Ar $r > R_1 + R_2$, $F^{(0)} = \frac{1}{r}$, $F^{1}_{i\lambda} = \frac{3}{2\lambda+1} \frac{R_i^{\lambda}}{r^{\lambda i}}$, $F^{2}_{i\lambda=2} = \frac{6}{5} \frac{R_i^2}{r^3}$, $F^{(2)}_{i\lambda=4} = \frac{R_i^4}{r^5}$. At shorter values of r , when nuclear surfaces overlap, there are more complicated expressions for the form-factors $F_{\lambda}^{(n)}(r)$. It is not important here because $R_C^B > R_1 + R_2$. Usually nuclei have quadrupole and hexadecapole static deformations $(\lambda = 2,4)$.

The short-range nuclear interaction depends on a distance between nuclear surfaces $\xi = r - R_1(\vec{\beta}_1, \theta_1) - R_2(\vec{\beta}_2, \theta_2)$, see Fig. 2. Woods-Saxon potential is often used to describe this interaction:

$$V_{ws}(\xi) = \frac{V_0}{1 + \exp(\zeta / a)}$$

where $\zeta = r - R_V - \Delta R_1 - \Delta R_2$, $\Delta R_1 = R_1(\dot{\beta}_1, \theta_1) - R_1$, and $\Delta R_2 = R_2(\dot{\beta}_2, \theta_2) - R_2$. “Proximity” potential is an another choice for parameterization of the nucleus-nucleus interaction [7]

$$V_{prox}(\xi) = 4\pi \gamma b P_{sph}^{-1} \cdot \Phi(\xi / \beta) \quad (6)$$

here $\Phi(\xi/\beta)$ is universal dimensionless form-factor, b is the thickness parameter of nuclear surface, γ is the surface stiffness, $\xi = r - R_1(\vec{\beta}_1, \theta_1) - R_2(\vec{\beta}_2, \theta_2)$, and $P_{sph} = 1/\bar{R}_1 + 1/\bar{R}_2$, where $\bar{R}_i = R_i[1 - (b/R_i)^2]$.

Attraction of two nuclear surfaces depends also on their curvatures. For deformed nuclei P_{sph} in (6) should be replaced by

$$P(\vec{\beta}_1, \theta_1, \vec{\beta}_2, \theta_2) = [(k_1^{\parallel} + k_2^{\parallel})(k_1^{\perp} + k_1^{\perp})]^{1/2} \quad (7)$$

where $k_i^{\parallel,\perp}$ are the principal local curvatures of the projectile and target.

The expression (7) may nominally reduce to zero at some negative deformations (touch of two planes). This non-physical effect originates due to neglecting the finite areas of the touching surfaces. Interactions of nearly located nucleons give the main contribution to the nucleus-nucleus potential energy. The number of such nucleons depends on the surface curvatures but it is always finite. Thus, instead of a simple replacement of P_{sph} by P in (6) , the expression

$$V_N = G(\vec{\beta}_1, \theta_1, \vec{\beta}_2, \theta_2) \cdot V_N^0(r; \vec{\beta}_1, \theta_1, \vec{\beta}_2, \theta_2)$$

is more appropriate, where V_N^0 is the nucleus-nucleus interaction calculated ignoring a change in surface curvatures and $G(\vec{\beta}_1, \theta_1, \vec{\beta}_2, \theta_2)$ is the geometrical factor, which

takes into account a change in the number of interacted nucleons (located in the nearest layers of two nuclei) comparing with spherical surfaces. The geometrical factor plays important role at large deformations [6].

The stiffness parameters C_λ could be calculated as follows [6]

$$C_\lambda = (2\lambda+1)\frac{\varepsilon_\lambda}{2\langle\beta_\lambda^0\rangle^2} \quad (8)$$

here $\varepsilon_\lambda = \hbar\omega_\lambda$ is the vibration energy, $\langle\beta_\lambda^0\rangle = \frac{4\pi}{3ZR_0^\lambda}\left[\frac{B(E\lambda)}{e^2}\right]^{1/2}$ is the RMS deformation of zero vibrations.

It is clear from (4) that the nucleus-nucleus interaction is a multi-dimensional potential energy surface. If several degrees of freedom are taken into account with subsequent consideration of the evolution of the nuclear system in multi-dimensional space, then the corresponding potential energy surface, which regulates this evolution, is usually called “driving potential”.

In Fig. 3.3 the potential energy of two initially spherical nuclei ^{40}Ca and ^{90}Zr is shown depending on their dynamic quadrupole deformation (for simplicity it is assumed here that the deformation energies of the two nuclei are proportional to their masses and, instead of two deformation parameters β_1 and β_2, only one $\beta = \beta_1 + \beta_2$ is used).

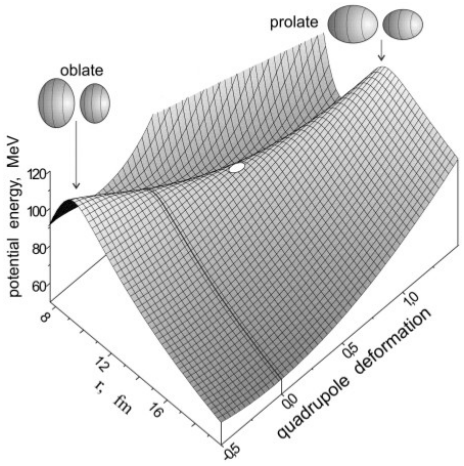

Fig. 3.3 Potential energy surface of the $^{40}Ca + ^{90}Zr$ interaction depending on quadrupole dynamic deformations of two nuclei. The minimal value of the fusion barrier (saddle point) is marked by the open circle.

The plots demonstrate the multi-dimensional character of the nucleus-nucleus interaction and of potential barrier. As can be seen, it is impossible to characterize the potential barrier by a specific value B of its height. Instead there is some continuous barrier distribution $F(B)$.

Barrier distribution function

The resent very precise experiments on near-barrier fusion reactions give a possibility to determine rather accurately the second derivative of $E\sigma_{fus}(E)$, which in classical limit may be identified with the so called "barrier distribution function" [8]

$$D(B)=\frac{1}{\pi R_B^2}d^2(E\sigma_{fus})/dE^2|_{E=B} \quad (9)$$

The structure of the function $D(B)$ (different for different pairs of nuclei) was found testifying to complicated dynamics of penetration of the potential barrier taking place in strong channel coupling condition.

Penetrability of one-dimensional barrier is defined by the well-known Hill-Wheeler formula (2). In that case the penetration probability $T_l(B,E)$ depends not arbitrary on B and l, but it is a function of the argument

$$x=B+\frac{\hbar^2}{2\mu R_B^2}l(l+1)-E \ ,$$

i.e., $T_l(B;E)=f(x)$. Using expression (1) for the fusion cross section, one may write

$$\frac{dE(\sigma_{fus})}{dE}=\frac{\pi\hbar^2}{2\mu E}\sum_{l=0}^{\infty}(2l+1)\frac{dT_l(B;E)}{dE} \quad (10)$$

Because

$$\frac{dT}{dE}=-\frac{dT}{dx}=-\frac{dT}{dl}\left(\frac{dx}{dl}\right)^{-1}=-\frac{dT}{dl}\frac{2\mu R_B^2}{\hbar^2}\frac{1}{2l+1} \ ,$$

then

$$\frac{d(E\sigma_{fus})}{dE}=-\pi R_B^2\sum_{l=0}^{\infty}\frac{dT_l(B;E)}{dl}$$

In collision of heavy nuclei many partial waves contribute to the fusion cross section, $T_l(B;E)$ is a smooth function of l, and summation in (10) may be replaced by the integration over l. This integral can be easily calculated giving ,

$$d(E\sigma_{fus})/dE\approx\pi R_B^2\cdot T_{l=0}(B;E) \quad \text{or}$$

$$D(E)\approx\frac{dT_{l=0}(B;E)}{dE}$$

In classical limit $T(E)=1$ at $E>B$ and $T(E)=0$ at $E<B$, i.e., $D(E)=\delta(E-B)$. In quantum case the penetration probability is given by (2) and the function $D(E)$ has one maximum at $E=B$ with the width

$$\hbar\omega_B\ln(17+12\sqrt{2})/2\pi\approx 0.56\,\hbar\omega_B$$

(for parabolic barrier). In real case the nucleus-nucleus potential energy is a multi-

dimensional surface, and the incoming flux overcomes the Coulomb barrier at different values of its height B (different values of dynamic deformations and/or orientations). In [2] the semi-empirical channel coupling model has been proposed for a simple estimation of multi-dimensional barrier penetrability basing on the idea of the "barrier distribution function". There are two cases: (I) fusion reactions involving spherical nuclei and (II) reactions with statically deformed nuclei.

Empirical Channel Coupling Model

The empirical channel coupling model was proposed by V. I. Zagrebaev [2]. The model considers two different cases: fusion of spherical and deformed nuclei in their ground states.

I Coupling to vibrational states (fusion of spherical nuclei)

Near-barrier fusion of spherical nuclei strongly depends on coupling of their relative motion to surface vibrations. In this case the Coulomb barrier depends on dynamic deformations. The total penetration probability should be averaged over barrier height B , and instead of (2) one may write

$$T_l(E)=\int F(B)\,T_l^{HW}[B(\beta);E]\,dB \quad (11)$$

where the normalized function $F(B)$ may be approximated by symmetric Gaussian

$$F(B)=N\cdot\exp\left(-\left[\frac{B-B_0}{\Delta_B}\right]^2\right) \quad (12)$$

located at $B_0=(B_1+B_2)/2$ and having the width $\Delta_B=(B_1-B_2)/2$. The value of quantity B_1 corresponds to minimal value of the two-dimensional barrier depended on dynamic deformation and B_2 defined as the Coulomb barrier of spherical nuclei. For very heavy nuclei, when the difference (B_2-B_1) is rather large, an asymmetric Gaussian with slightly less "inner" width $(\Delta_B^1\le\Delta_B^2)$ approximates better the function $F(B)$ [2].

II Coupling to rotational states (fusion of statically deformed nuclei)

For statically deformed nuclei the penetration probability should be averaged over the orientations of both nuclei. In this case the total penetration probability is given by

$$T_l(E)=\frac{1}{4}\int_0^{\pi}\int_0^{\pi} T_l^{HW}[B(\vec{\beta}_1,\theta_1,\vec{\beta}_2,\theta_2);E]\sin\theta_1\sin\theta_2\,d\theta_1\,d\theta_2 \quad (13)$$

where $B(\vec{\beta}_1,\theta_1,\vec{\beta}_2,\theta_2)$ is the orientation dependent barrier β_1 and β_2 are the static deformation parameters of interacting nuclei.

Quantum Channel Coupling Model [6,9]

Hamiltonian of two deformable nuclei rotating in reaction plane is written as

$$H=-\frac{\hbar^2\Delta_r^2}{2\mu}+V_C(r;\vec{\beta}_1,\theta_1,\vec{\beta}_2,\theta_2)+V_N(r;\vec{\beta}_1,\theta_1,\vec{\beta}_2,\theta_2)+\sum_{i=1,2}\frac{\hbar^2\hat{I}_i^2}{2J_i}+ \\ +\sum_{i=1,2}\sum_{\lambda\geq 2}\left(-\frac{1}{2d_{i\lambda}}\frac{\partial^2}{\partial s_{i\lambda}^2}+\frac{1}{2}c_{i\lambda}s_{i\lambda}^2\right) \quad (14)$$

where J_i are the moments of inertia. Decomposing the total wave function over the partial waves

$$\Psi_{\vec{k}}(r,\vartheta,\vec{\alpha})=\frac{1}{kr}\sum_{l=0}^{\infty}i^l e^{i\sigma_l}(2l+1)\chi_l(r,\vec{\alpha})P_l(\cos\vartheta) \quad (15)$$

one get the following set of the coupled Schrodinger equations

$$\frac{\partial^2}{\partial r^2}\chi_l(r,\vec{\alpha})-\frac{l(l+1)}{r^2}\chi_l(r,\vec{\alpha})+\frac{2\mu}{\hbar^2}[E-V(r,\vec{\alpha})-\hat{H}_{int}(\vec{\alpha})]\chi_l(r,\vec{\alpha})=0 \quad (16)$$

Here α are the internal degrees of freedom (deformations and/or angles of rotation)), $H_{int}(\vec{\alpha})$ is the corresponding Hamiltonian, and $V(r,\vec{\alpha})=V_c(r,\vec{\alpha})+V_N(r,\vec{\alpha})$. The functions $\chi_l(r,\vec{\alpha})$ may be also decomposed over the complete set of the eigenfunctions of the Hamiltonian $H_{int}(\vec{\alpha})$

$$\chi_l(r,\vec{\alpha})=\sum_V y_{l,v}(r)\cdot\varphi_v(\vec{\alpha}) \quad (17)$$

and the radial wave functions $y_{l,v}(r)$ satisfy a set of differential equations solved numerically

$$y_{l,v}''-\frac{l(l+1)}{r^2}y_{l,v}+\frac{2\mu}{\hbar^2}[E_v-V_{vv}(r)]y_{l,v}-\sum_{\mu\neq v}\frac{2\mu}{\hbar^2}V_{v\mu}(r)y_{l,\mu}=0 \quad (18)$$

Here $E_v=E-\varepsilon_v$, ε_v is the nucleus excitation energy in the channel v , and $V_{v\mu}(r)=\langle\varphi_v|V(r,\vec{\alpha})|\varphi_\mu\rangle$ is the coupling matrix.

At low energies, not so heavy colliding nuclei having overcome the Coulomb barrier and coming in contact fuse (i.e., form a compound mono-nucleus) with a probability close to unity. The fusion cross section can be measured in that case by detecting all the fission fragments and evaporation residues. Thus, formulating the boundary conditions for the wave function $\Psi_{\vec{k}}(r,\vartheta,\vec{\alpha})$ it is usually assumed that the flux, which overcomes the Coulomb barrier, is absorbed completely (forming the compound nucleus) and is not reflected from the inner region. It means that at

$r < R_{fus} \approx R_1 + R_2$ the functions $\chi_l(r, \vec{\alpha})$ are incoming waves and have not outgoing components reflected from the region $0 \le r \le R_{fus}$. The details of satisfying this boundary condition can be found in [6].

At large distances $(r \to \infty)$ the wave function has an ordinary behavior of scattering wave: incoming and outgoing waves in the elastic channel $v = 0$, and outgoing waves in all other channels. For the partial wave functions this corresponds to the condition

$$y_{l,v}(r \to \infty) = \frac{i}{2}\left[h_l^{(-)}(\eta_v, k_v r) \cdot \delta_{v0} - \left(\frac{k_0}{k_v}\right)^{1/2} S^l_{v0} \cdot h_l^{(+)}(\eta_v, k_v r) \right] \quad (19)$$

where $k_v^2 = \frac{2\mu}{\hbar^2} E_v$, $\eta_v = \frac{k_v Z_1 Z_2 e^2}{2E_v}$ is the Sommerfeld parameter, $\sigma_{l,v} = arg\,\Gamma(l+1+i\eta_v)$ is the Coulomb partial phase shift, $h_l^{(\pm)}(\eta_v, k_v r)$ are the Coulomb partial wave functions with the asymptotic behavior $\exp(\pm i x_{l,v})$, $x_{l,v} = k_v r - \eta_v \ln 2k_v r + \sigma_{l,v} - l\pi/2$, S^l_{v0} are the partial scattering matrix elements. Similar expression is obtained for the closed channels $(E_v < 0)$ with imaginary argument of the function $h_l^{(+)}(\eta_v, k_v r)$.

The fusion cross section calculated within channel coupling approach is defined by the same expression (1), where the partial transmission coefficients are defined by the ratio of the passed (absorbed) and incoming flaxes

$$T_l(E) = \sum_v \frac{j_{l,v}}{j_0} \quad (20)$$

Here

$$j_{l,v} = -i\frac{h}{2\mu}\left(y_{l,v}\frac{dy^*_{l,v}}{dr} - y^*_{l,v}\frac{dy_{l,v}}{dr} \right)\Big|_{r \le R_{fus}}$$

is the partial flux in the channel v , and $j_0 = \hbar k_0/\mu$.

4. Results

We chose the well-studied reaction $^{40}Ca + ^{90}Zr$ as an object of research [10]. These nuclei are spherical, and consequently, the vibrational degrees of freedom have a significant effect on the fusion cross section. The vibrational properties of ^{40}Ca and ^{90}Zr are presented in Table 1.

TABLE 1 The characteristics of ^{40}Ca and ^{90}Zr

Empirical Channel Coupling Model

$V_0^{vol} = -73\ MeV$	$r_0^{vol} = 1.18\ fm$
$r_0^{coul} = 1.12\ fm$	$a_0^{vol} = 0.67\ fm$

	^{40}Ca	^{90}Zr
λ	3-	3-
$\hbar\omega$	3.7	2.7
C	2.5	2

Quantum Channel Coupling Model.

	^{40}Ca	^{90}Zr	
λ	3-	2+	3-
$\hbar\omega$	3.7	2.1	2.7
β	0.41	0.08	0.21

The experimental fusion cross section and experimental evaluation of the barrier distribution function are shown in fig. 4.1. It can be seen that the barrier distribution function has two well-defined peaks. These peaks are due to the coupling of the relative motion with vibrational degrees of freedom.

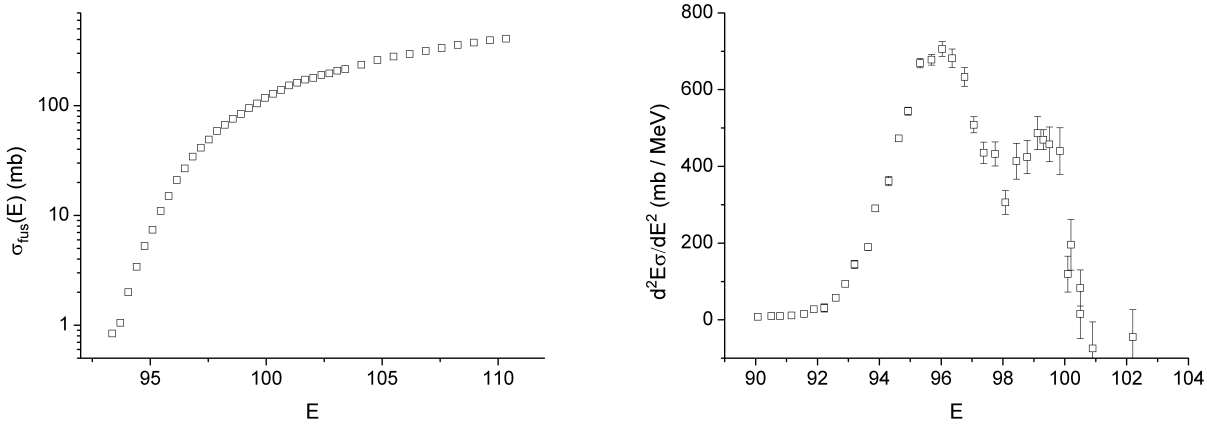

Figure 4.1. The experimental fusion cross section and barrier distribution function for $^{40}Ca + ^{90}Zr$ [10].

For the chosen pair of nuclei the octupole vibrations ($\lambda=3$) should have a largest effect on the sub-barrier fusion. Figure 4.2 shows analysis of the $^{40}Ca+^{90}Zr$ fusion reaction within the ECC and QCC models. The calculation are done with the Woods-Saxon nucleus-nucleus potential with the following parameters: $V_0=-73\,MeV$, $r_0=1.18\,fm$, $a=0.67\,fm$.

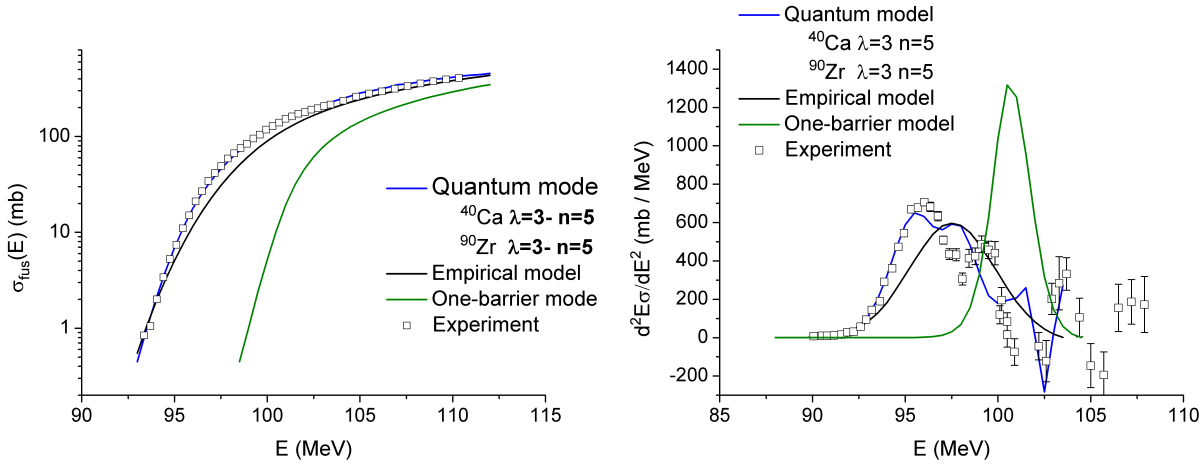

Figure 4.2. The fusion cross section and the barrier distribution function from a different models in comparison with experiment. 10 vibrational phonons are included into the QQC calculations.

As can be seen from the Fig. 4.2. the single-barrier penetration model does not agree with experiment. The ECC model is more consistent with the experiment. The maximum is shifted towards lower energies (comparing to the single-barrier model) and the barrier distribution is wider, but the structure of the barrier distribution function is not reproduced. The QCC model reproduces the structure of the barrier distribution function, as well as the fusion cross section at near-barrier energies.

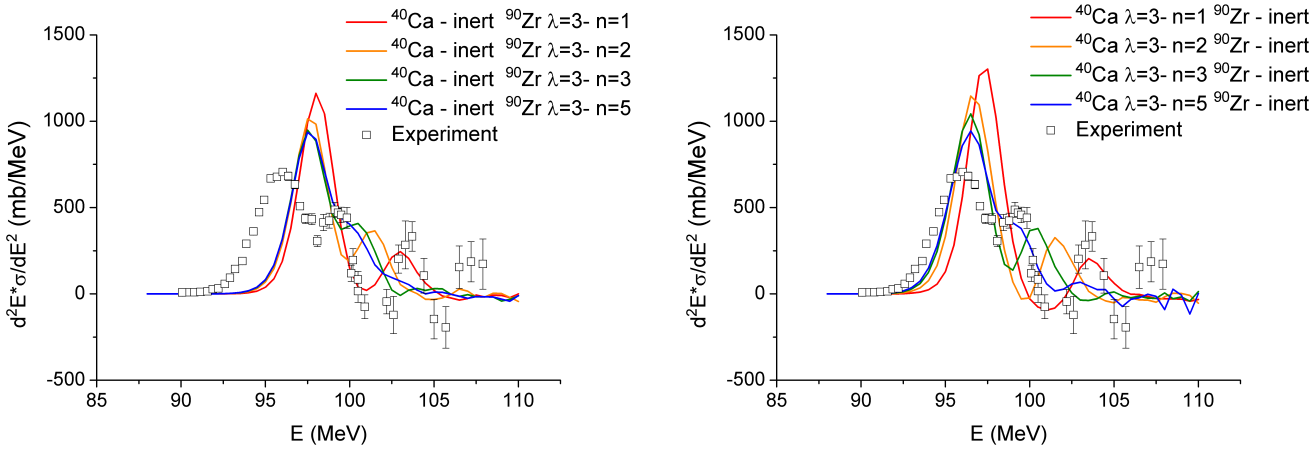

Figure 4.3. The influence of vibrational degree of freedom of each nucleus on the barrier distribution function.

The next step in our analysis is the study of influence of different vibrational modes on the sub-barrier fusion. The result shown in Fig.4.3. The calculations are done for the barrier distribution function with different number of phonons (n) included to the QCC model. As can be seen from the figure, the octupole vibrational degree of freedom of ^{40}Ca have a major influence on the barrier distribution function. One may notice this by comparing the calculated values at lower energies with the experimental data.

The influence of phonons number on barrier distribution function is studied further. The result are shown in fig.4.4.

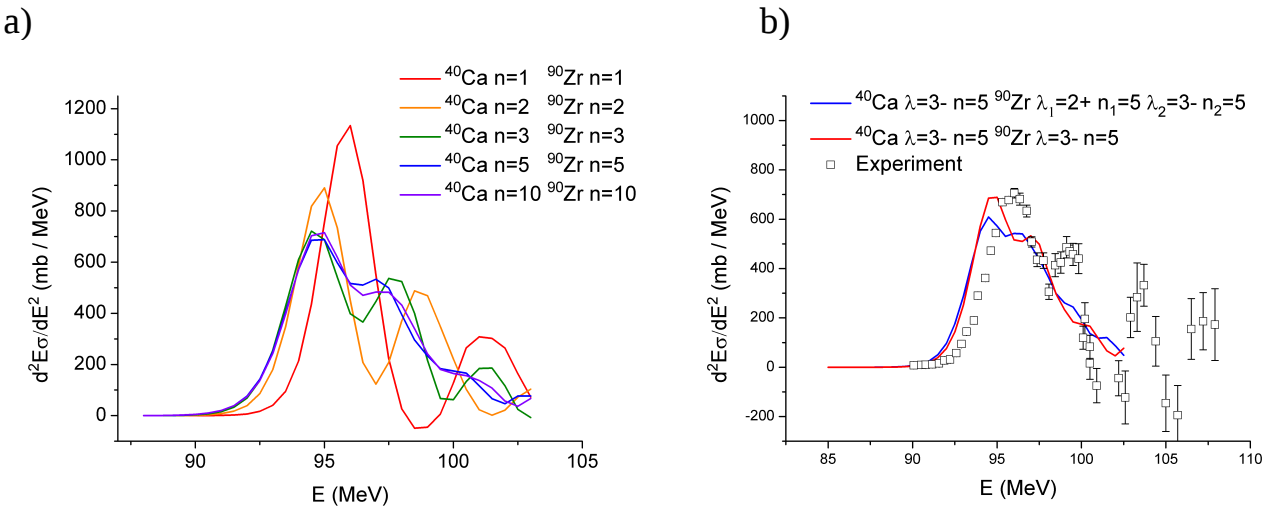

Figure 4.4. The influence of phonon number a) and additional mode b) on the barrier distribution function.

As can be seen from the Fig. 4.4 a), the barrier distribution function smooths when the phonon number increases. The barrier distribution function changes slightly when phonons number is greater than 5, i.e. it reaches its asymptotic at $n \approx 5$. However, the structure of barrier distribution function remains when a large number of phonons is considered in the QCC calculations. Figure 4.4 b) shows that the account for additional mode a slightly influences the barrier distribution function.

5. Conclusion

This work was focused on the theoretical analysis of the processes of near-barrier fusion on the example of the $^{40}Ca + ^{90}Zr$ system. In particular, we have analyzed the fusion cross section and the barrier distribution function. The calculations were performed with the use of the web knowledge base NRV [4]. Two models were employed, namely the empirical channel coupling model, and the quantum channel coupling model.

The barrier distribution function has two well-defined peaks. These peaks are due to the coupling of the relative motion with vibrational degrees of freedom. The single-barrier penetration model does not agree with experiment. The empirical channel

coupling model is more consistent with experiment. The maximum is shifted towards lower energies and the distribution is wider, but the structure of barrier distribution function is not reproduced. The quantum channel coupling model reproduces the structure of barrier distribution function, and one more accurately reproduced fusion cross section in near-barrier energies region. The optimum number of phonons that showed included into the QCC computational scheme is $\approx$ 5, since of this value both the fusion reach their asymptotical values.

REFERENCES

[1] M. Beckerman, Rep. Prog. Phys., 51 (1988) 1047
[2] V.I. Zagrebaev, Phys.Rev., C 64 (2001) 034606
V.I. Zagrebaev et al., Phys.Rev., C 65 (2002) 014607
[3] M.Dasgupta D.J. Hinde, Annu. Rev. Nucl. Part. Sci. 48 (1998) 401-61
[4] http://nrv.jinr.ru
[5] D.L. Hill, J.A. Wheeler, Phys.Rev., 89 (1953) 1102
[6] V.I. Zagrebaev and V.V. Samarin, Yad. Fiz., 67, No.8 (2004) 1488
[7] J. Blocki, J. Randrup, W.J. Swiatecki, C.F. Tsang, Ann.Phys.(N.Y.), 105 (1977) 427
[8] N. Rowley, G.R. Satchler, P.H. Stelson, Phys.Lett., B 254 (1991) 25
[9] K.Hagino, N.Rowley, A.T.Kruppa, Comp.Phys.Commun., 123 (1999) 143
[10] H. Timmers, D. Ackermann, S. Beghini, et al., Nucl. Phys. A 633 (1998) 421